ADVANCED FUNCTIONAL MATERIALS
www.afm-journal.de

Materials Views
www.MaterialsViews.com

In Situ Fully Light-Driven Switching of Superhydrophobic Adhesion

*Chao Li, Yuanyuan Zhang, Jie Ju, Futao Cheng, Mingjie Liu, Lei Jiang, and Yanlei Yu**

An in situ fully light-driven switching of superhydrophobic adhesion is demonstrated based on simply spin-coating a hydrophobic azo-polymer on an optimized micro-nanopost arrayed silicon substrate. Furthermore, the detailed designing principles are discussed, which might shed light on efficient exploitation of superhydrophobic liquid/solid interfaces for smart microfluidic control.

1. Introduction

Liquid–solid adhesion, due to its great interest for both fundamental research and practical applications, has been widely investigated.[1] In common cases, a single performance of adhesion at liquid/solid interfaces such as ultralow adhesive or high adhesive is just needed,[2–6] while in some other specific cases, e.g., no-loss microdroplet transfer,[7] reversible switching of adhesion is expected.[8–10] In particular, in situ control of liquid-solid adhesion, i.e., at least one cycle of the on-off operations is maneuvered with the same liquid-solid interface,[11] is of significant value for design of novel microfluidic devices. However, until now in situ or real-time manipulation of water droplet adhesion on superhydrophobic surfaces in non-contact stimuli mode has not been reported.

2. Results and Discussion

2.1. Design and Preparation of Azo-Polymer-Coated Superhydrophobic Surfaces

It is well-known that both wettability and adhesion of interfaces greatly depend on the cooperation of surface chemical composition and morphological roughness.[12–17] As to realization and regulation of superhydrophobic adhesion, relatively low surface energy and micro-nano binary morphology are, in general, necessary. More importantly, stimuli-responsive factors must be introduced,[18] either reversibly changing surface chemical composition, morphological roughness, or both. Directed by the above principles, a strategy for in situ light-driven switching of superhydrophobic adhesion was performed and carefully optimized (**Figure 1**). Firstly, a micro-nanopost arrayed silicon wafer with a semiquantitative surface roughness was prepared by utilizing photolithography and chemical etching.[19] Then, a side-chain azo-polymer (PA8AB6, poly[4-(8-acryloyloxy) octyloxy-4′-hexyloxy] azobenzene) was synthesized and spin-coated on the surface as a light-responsive coating[20] (see details in Part S1 of the Supporting Information). To improve the uniformity of the azo-polymer coating, it should be noted that a transitional layer of cyclized rubber negative photoresist (SZ2; the chemical structure of its main component is shown in Figure S2 of the Supporting Information) was introduced between the light-responsive

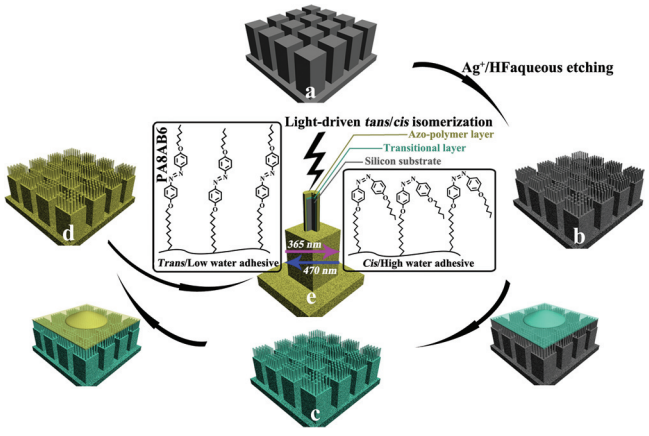

Figure 1. Schematic illustration of the preparation process of the micro-nano complex azo-polymer coating and the light-driven *trans*/*cis* isomerization. a) Micropost-arrayed silicon wafer prepared by photolithography. b) Micro-nanopost-arrayed silicon wafer obtained by chemical (Ag^+/HF acid) etching of the wafer in (a). c) Micro-nanopost-arrayed silicon wafer with transitional coating (SZ2). The transitional layer is introduced to improve the film uniformity of the azo-polymer on silicon wafer. d) Micro-nanopost-arrayed silicon wafer with azo-polymer coating (PA8AB6). e) Sectional view of a single silicon post after spin-coated successively with SZ2 and PA8AB6. Inset: representative picture of *trans*/*cis* photoisomerization of the azobenzene groups at surface.

C. Li, Y. Y. Zhang, F. T. Cheng, Prof. Y. L. Yu
Department of Materials Science
Fudan University
Shanghai 200433, P. R. China
E-mail: ylyu@fudan.edu.cn
C. Li, J. Ju, M. J. Liu, Prof. L. Jiang
Beijing National Laboratory for Molecular Sciences (BNLMS)
Institute of Chemistry
Chinese Academy of Sciences
Beijing 100190, P. R. China
Prof. L. Jiang
School of Chemistry and Environment
Beijing University of Aeronautics and Astronautics
Beijing 100191, P. R. China

DOI: 10.1002/adfm.201101922

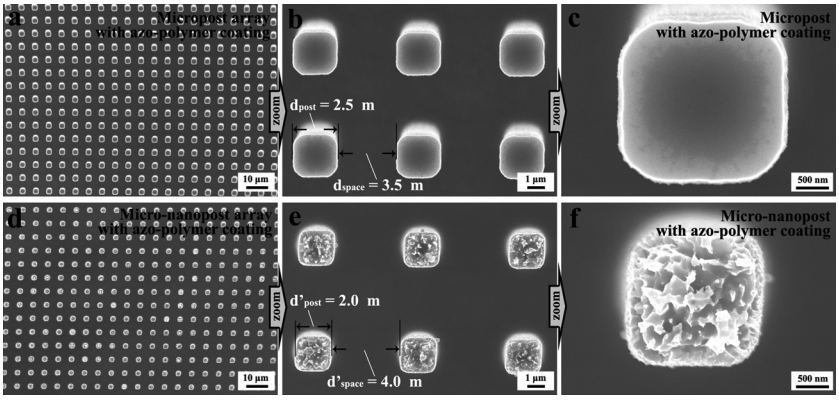

Figure 2. SEM images of the morphologies of the substrates with azo-polymer coating. a–c) Micropost array with azo-polymer coating. d–f) Micro-nanopost array with azo-polymer coating. The structural parameters of the micropost array after coating are: the width of post, d_{post} = 2.5 μm; the spacing between two nearest posts, d_{space} = 3.5 μm. After etching and coating, the structural parameters of the micro-nanopost array change to: d'_{post} = 2.0 μm, d'_{space} = 4.0 μm. The average scale of the nanostructures etched on the microposts is less than 100 nm.

coating and the silicon substrate, which was treated to crosslink with UV light irradiation after coated on the silicon substrate. From the observation by scanning electron microcopy (SEM), the coatings on both micropost- and micro-nanopost-arrayed silicon wafers are uniform, and the surface micro-nanostructures are well maintained (**Figure 2**).

2.2. Photoresponsive Static and Dynamic Wettability

Subsequently, photoresponse of the azo-polymer coatings was confirmed by ultraviolet-visible (UV-vis) spectroscopy and contact angle (CA)/contact angle hysteresis (CAH) measurements (see details in Part S2 of the Supporting Information). With an alternating irradiation of UV and visible light, the azo-polymer coatings show a *trans*/*cis* photoisomerization, which leads to a reversible change both in static and dynamic contact angles. Besides the polarity change of the coatings, surface roughness change might also occur and contribute to the wettability switching. To investigate the light-induced fluctuation of the azo-polymer coatings, in situ atomic force microscopy (AFM) characterization was performed (**Figure 3**). In the *trans* state, the coatings are relatively smooth with an average surface roughness (Box R_a, where Box means a selected data cell) about 0.45 nm. In contrast, in *cis* state, the coatings become a little rougher with a Box R_a about 0.75 nm. The amplitude of Box R_a (about 3 Å) denotes that the azobenzene side chains are in a random orientation on the substrates' surface.[21,22] Moreover, it also reveals here that the main contribution of the *trans*/*cis* photoisomerization of the azobenzene groups is surface polarity changing rather than roughness.

To a certain composition of liquid droplet (e.g., water) and a fixed third phase (e.g., air), superhydrophobic adhesion is directly determined by liquid/solid interfacial contact area (ICA) and gas-liquid-solid three-phase contact line (TCL).[23–25] As to whether a droplet can roll off from the substrate, it also depends on the comparison between adhesive force (AF) and the component of droplet's self-gravity ($G_{droplet}$) along the tilt plane of the substrate.[26] In order to make an assessment for the regulation ability of superhydrophobic adhesion, we propose here a definition of AF or $G_{droplet}$ grasp-release window (GRW_{AF} or $GRWG_{droplet}$) that means the difference of AF or $G_{droplet}$ between the maximum grasp and minimum release states. For GRW_{AF}, it should be noted that the AF for preventing droplet's rolling is smaller than that for preventing droplet's separating because rolling the droplet only needs to

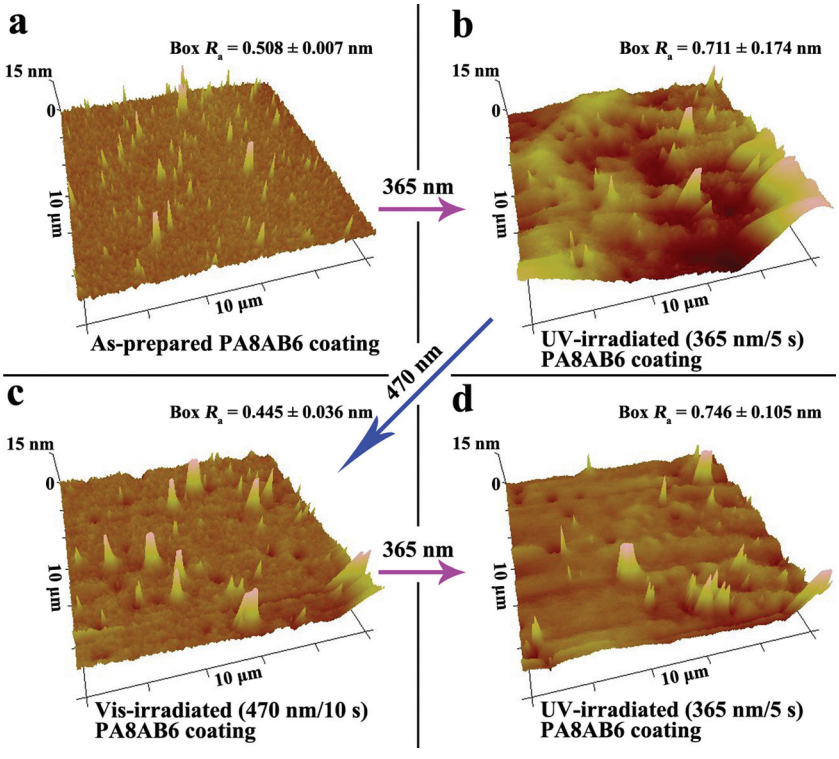

Figure 3. In situ AFM height images of PA8AB6 coating upon light irradiation. a) The as-prepared PA8AB6 coating. b) UV-irradiated (365 nm, 120 mW cm^{-2}, 5 s) PA8AB6 coating. c) Visible-light-irradiated (470 nm, 30 mW cm^{-2}, 10 s) PA8AB6 coating. d) Secondary UV-irradiated (365 nm, 120 mW cm^{-2}, 5 s) PA8AB6 coating. The scanning size of all the four images is 10 μm × 10 μm. From (a–d), the results of average surface roughness (Box R_a) are 0.508 ± 0.007 nm, 0.711 ± 0.174 nm, 0.445 ± 0.036 nm, and 0.746 ± 0.105 nm, respectively. With the alternating UV-vis irradiation, the surface roughness is alternately varied between relatively rough and relatively smooth. The amplitude of Box R_a is about 3 Å, which corresponds to the *trans*/*cis* photoisomerization of the azobenzene groups at surface.

overcome the AF generated by the TCL at the receding part.[25,27] For GRW$G_{droplet}$, it should correspond to a certain tilt angle of the substrate.

In the following parts, we use GRW_{AF} to estimate the regulation ability of superhydrophobic adhesion. It is easy to imagine that for one system if GRW_{AF} is too narrow compared with AF, the regulation effect might be not obvious and easy to be disturbed. This point is reflected in the control experiment on the micropost-arrayed silicon wafer with azo-polymer coating. Due to both the relatively larger ICA and TCL of the micropost array (which leads to a larger AF), independent of if the water droplets are larger (>2 μL, not shown) or smaller (≤2 μL), the light-stimuli effect is small (see details in Part S3 of the Supporting Information). Thus, the AF should be decreased to a certain level to have a match with the GRW_{AF} caused by alternating UV-vis irradiation. The strategy for solving this issue is to introduce nanostructures on the original microposts. The resulting micro-nano binary structures make the ICA much smaller and the TCL much more discontinuous, which might greatly lower the AF.

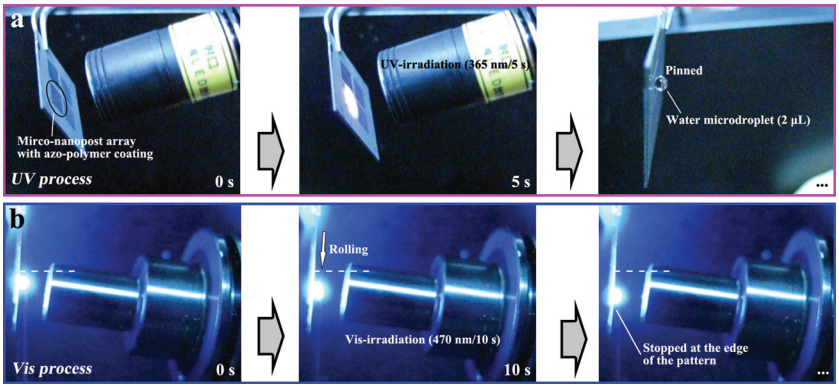

Figure 4. In situ light-controlled switching of superhydrophobic adhesion on micro-nanopost array with azo-polymer coating. a) UV process. The micro-nanopost array was firstly irradiated by UV light (365 nm, 120 mW cm^{-2}) for 5 s and a 2 μL water droplet can be pinned on the array poised vertically. b) Vis process. After the UV process, the pinned water droplet was irradiated with visible light (470 nm, 30 mW cm^{-2}). For 10 s, the pinned water droplet rolls off. The white dash line in each photograph in (b) shows the initial position of the pinned water droplet.

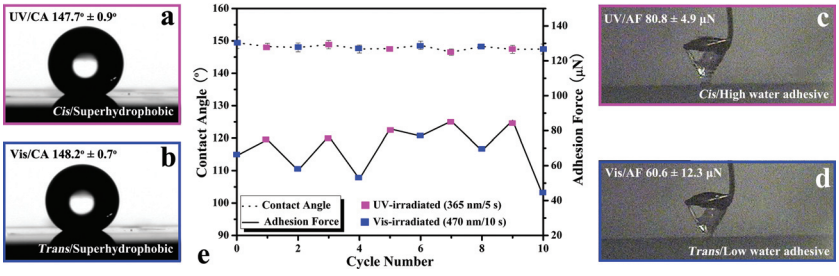

Figure 5. Photoinduced changes of superhydrophobic adhesion on micro-nanopost array with azo-polymer coating. a) Profile of the water droplet on the array after UV light irradiation. The water droplet is in superhydrophobic state (the average CA, 147.7° ± 0.9°). b) Profile of the water droplet on the array after visible light irradiation. The water droplet is in superhydrophobic state (the average CA, 148.2° ± 0.7°). c) Optical image of the maximum-deformed water droplet on the array after UV light irradiation. The surface is in *cis* state, which shows high water adhesion (the average AF, 80.8 ± 4.9 μN). d) Optical image of the maximum-deformed water droplet on the array after visible light irradiation. The surface is in *trans* state, which shows low water adhesion (the average AF, 60.6 ± 12.3 μN). e) CA and AF results with alternating UV-vis irradiation (five cycles).

2.3. In Situ Switching of Superhydrophobic Adhesion Driven by Light

With the above optimization, a 2 μL water droplet can be pinned on the micro-nanopost array after UV light irradiation (**Figure 4**a, **Figure 5**a). Then, after visible light irradiation for about 10 s, the pinned droplet rolls off (Figure 4b, Figure 5b, and the movie in the Supporting Information). The AF is obviously decreased compared with that of the micropost array (Figure 5c,d). Moreover, the GRW_{AF} generated by UV-vis irradiation is about 20.2 μN, which is enlarged to 25.0% and 33.3% of the minimum and maximum AFs, respectively (Figure 5e). This is the basis for realization of the in situ fully light-driven switching of superhydrophobic adhesion. But, it should be noted that the GRW_{AF} of this system is still not large enough for maneuvering larger or smaller water droplet than 2 μL. Armed with both the theoretical and experimental analyses, an ideal large GRW might be obtained by reversible change of morphological roughness with external stimuli. The related works for an enlarged light-responsive GRW are ongoing.

3. Conclusions

In conclusion, by an optimization of azo-polymer coating on silicon substrate with micro-nano binary structures, in situ fully light-driven switching of superhydrophobic adhesion to water droplet has been realized. This kind of non-contact real-time controllable switching of microdroplet's adhesion might inspire and facilitate the designs and applications in novel microfluidic devices, e.g., remote-controlled valve, sensor, mechanical hand, microreactor, and so on. Moreover, the design principles disclosed in this work shall be a guidepost for the following researches on smart liquid/solid interfaces with on-off switching of superhydrophobic adhesion.

4. Experimental Section

Methods: Detailed chemicals and sample preparations are included in the Supporting Information (Part S1). Attenuated total reflection infrared (ATR-IR) spectra of the coatings (SZ2, SZ2 and PA8AB6) were recorded on a Bruker EQUINOX 55. UV-vis spectra were collected using a Hitachi U-3010 spectrophotometer. The corresponding sample was spin-coated on a quartz slide (1 mm thick). AFM tapping mode images were acquired using an atomic force microscope (NanoScope IIIa MultiMode,

Veeco Instruments). The set-point amplitude ratio was adjusted to be 0.7–0.9. Si tips (TESP, Digital Instruments) with a resonance frequency of approximately 300 kHz and a spring constant of about 40 N m^{-1} were used. Morphologies of the spin-coated silicon wafers were characterized by SEM (Hitachi S-4800) under the accelerating voltage of 10 kV. CA and CAH were measured on a contact angle system OCA20 (DataPhysics, Germany). AF measurements were performed on Dataphysics DCAT11 (see details in Part S4 in the Supporting Information). The step rate of the sample plate was set as 0.01 mm s^{-1}. Because the size of water droplet can affect, in particular, its mobility on a certain surface, the droplet size should be tailored to realize the in situ switching of superhydrophobic adhesion. Using a primary optimization of the droplet size (not shown), 2 μL was finally fixed for demonstration. The average CA and AF values were obtained by measuring the same sample at least in five different positions. 18 MΩ cm deionized water (Millipore Milli-Q (0.22 μm)) was used for all the wettability and adhesion characterizations. The light intensities of the UV light-emitting diode (LED) (OMRON ZUV-C30H, 365 nm) and the vis-LED (CCS HLV-24, 470 nm) for irradiation were 120 mW cm^{-2} and 30 mW cm^{-2}, respectively. All the measurements were conducted at room temperature (23 °C).

Supporting Information

Supporting Information is available from the Wiley Online Library or from the author.

Acknowledgements

This article was amended on February 22, 2012 to include an author affiliation that was not present in the version originally published online. The authors are grateful for financial support from NSFC (21134003, 20920102036, 20974113, 50873028), the National Research Fund for Fundamental Key Projects (2011CB935700, 2010CB934700, 2009CB930400, 2007CB936403), DPHE (20100071110014), PCSIRT (IRT0911), and Shanghai Rising-Star Program (11QH1400400).

Received: August 16, 2011
Revised: November 10, 2011
Published online: December 16, 2011

[1] M. J. Liu, Y. M. Zheng, J. Zhai, L. Jiang, *Acc. Chem. Res.* **2010**, *43*, 368.
[2] R. Blossey, *Nat. Mater.* **2003**, *2*, 301.
[3] K. Koch, B. Bhushan, Y. C. Jung, W. Barthlott, *Soft Matter* **2009**, *5*, 1386.
[4] D. Quéré, *Rep. Prog. Phys.* **2005**, *68*, 2495.
[5] M. H. Jin, X. J. Feng, L. Feng, T. L. Sun, J. Zhai, T. J. Li, L. Jiang, *Adv. Mater.* **2005**, *17*, 1977.
[6] F. M. Chang, S. J. Hong, Y. J. Sheng, H. K. Tsao, *Appl. Phys. Lett.* **2009**, *95*, 064102.
[7] X. Hong, X. F. Gao, L. Jiang, *J. Am. Chem. Soc.* **2007**, *129*, 1478.
[8] C. Li, R. W. Guo, X. Jiang, S. X. Hu, L. Li, X. Y. Cao, H. Yang, Y. L. Song, Y. M. Ma, L. Jiang, *Adv. Mater.* **2009**, *21*, 4254.
[9] D. A. Wang, Y. Liu, X. J. Liu, F. Zhou, W. M. Liu, Q. J. Xue, *Chem. Commun.* **2009**, 7018.
[10] D. Wu, S. Z. Wu, Q. D. Chen, Y. L. Zhang, J. Yao, X. Yao, L. G. Niu, J. N. Wang, L. Jiang, H. B. Sun, *Adv. Mater.* **2011**, *23*, 545.
[11] M. Callies, D. Quéré, *Soft Matter* **2005**, *1*, 55.
[12] T. Onda, S. Shibuichi, N. Satoh, K. Tsujii, *Langmuir* **1996**, *12*, 2125.
[13] Z. Yoshimitsu, A. Nakajima, T. Watanabe, K. Hashimoto, *Langmuir* **2002**, *18*, 5818.
[14] C. W. Extrand, *Langmuir* **2004**, *20*, 5013.
[15] B. He, N. A. Patankar, J. Lee, *Langmuir* **2003**, *19*, 4999.
[16] A. Marmur, *Langmuir* **2003**, *19*, 8343.
[17] A. Lafuma, D. Quéré, *Nat. Mater.* **2003**, *2*, 457.
[18] L. Jiang, R. Wang, B. Yang, T. J. Li, D. A. Tryk, A. Fujishima, K. Hashimoto, D. B. Zhu, *Pure Appl. Chem.* **2000**, *72*, 73.
[19] T. L. Sun, G. J. Wang, L. Feng, B. Q. Liu, Y. M. Ma, L. Jiang, D. B. Zhu, *Angew. Chem.* **2004**, *116*, 361; *Angew. Chem. Int. Ed.* **2004**, *43*, 357.
[20] A. S. Angeloni, D. Caretti, C. Carlini, E. Chiellini, G. Galli, A. Altomare, A. Solaro, M. Laus, *Liq. Cryst.* **1989**, *4*, 513.
[21] J. M. Mativetsky, G. Pace, M. Elbing, M. A. Rampi, M. Mayor, P. Samori, *J. Am. Chem. Soc.* **2008**, *130*, 9192.
[22] M. E. Garah, F. Palmino, F. Cherioux, *Langmuir* **2010**, *26*, 943.
[23] N. A. Patankar, *Langmuir* **2004**, *20*, 7097.
[24] C. W. Extrand, *Langmuir* **2002**, *18*, 7991.
[25] C. Dorrer, J. Rühe, *Langmuir* **2006**, *22*, 7652.
[26] M. Miwa, A. Nakajama, A. Fujishima, K. Hashimoto, T. Watanabe, *Langmuir* **2000**, *16*, 5754.
[27] L. C. Gao, T. McCarthy, *Langmuir* **2006**, *22*, 2966.